MICROSTRUCTURE AND OXIDATION BEHAVIOR OF THE OXIDE DISPERSION STRENGTHENED STAINLESS STEEL 316L WITH ZIRCONIA DISPERSION

Syahfandi Ahda[1], Rohmad Salam[1], Agus Sujatno[1], Diene Hairani[1], Nanda Shabrina[1], Sulistioso Giat[1], Bandriyana [1]

[1]Center for Science and Technology of Advanced Materials
National Nuclear Energy Agency
e-mail: bandri@batan.go.id.

ABSTRACT

Synthesis of the oxide dispersion sODS steels was performed by dispersing 0.5 wt % zirconia to the stainless steel SS 316L by the powder metallurgy method. The ball milling process was carried out for pre-alloying the elements continued with the consolidation performed by the compaction and sintering process using the APS (Arc Plasma Sintering). Analysis of microstructure was performed by observing the morphology, identify the phase and evaluate the oxide distribution. An oxidation test was carried out at 700°C for 8 hours using the MSB (Magnetic Suspension Balanced) apparatus to evaluate the primary oxidation curve. The same grain fineness consists of 2 dominant phases, so the presence of an austenitic phase and a ferritic phase has been analyzed from the X-Ray Diffraction pattern. The homogeneous distribution of zirconia was observed, followed by improvements in mechanical properties, which could be identified by hardness testing. The parabolic phenomenon oxidation curve was explained by the excellent high-temperature oxidation behaviour of the ODS steel, followed by the formation of ZrO_2 oxide protective thin layer.

INTRODUCTION

The corrosion resistance of austenitic stainless steel makes this material widely used in corrosive environments as a support material in the chemical industry, biomaterials industry, and others. It can even be a candidate for cladding material in nuclear fuel reprocessing plants. Therefore, as a cladding material in high-temperature reactors, it has been reported that the developed Oxide Dispersion-Strengthened (ODS) steel has high corrosion resistance with relatively good mechanical properties [1], [2].

As is well known, ferritic ODS steel was designed as the main candidate for cladding material for its excellent strength and in radiation attack, especially for swelling resistance [3], [4], [5]. Recently, some investigation revealed that austenitic ODS steel has more advantages than ferritic ODS steel for its better creep properties at high temperatures [6], [7]. However, the austenitic ODS steel mainly composes of fcc crystalline structure, has lower swelling and corrosion resistance that was dangerous in the cladding material.

Some research was conducted to improve the austenitic ODS steel behaviour by optimizing the composition and manufacturing process. The addition of zirconium in the ODS steel dispersed by Yttria (Y_2O_3) and also the use of zirconia (ZrO_2) as a dispersed to replace the Yttria showed increasing the corrosion of oxidation resistance behaviour [8], [9]. One of the main problems experienced in the fuel cladding was the material oxidation at high temperatures, mainly during accident conditions such as LOCA (Loss of Coolant Accident). Therefore, the high-temperature oxidation characteristic of cladding material should be determined to fulfil the safety requirement. This paper experimented with the high-temperature oxidation characteristic of the austenitic ODS alloy synthesized by dispersing the zirconia. Oxidation rates, formation of oxide layers, analysis of crystal structure content,

microstructure and mechanical changes due to zirconia dispersion in the process have been discussed.

.

METHODS

The sample alloy was synthesized by powder metallurgy method with austenitic steel SS 316L and ZrO_2 as dispersed. The materials were then milling for 20 hours then compacted with isostatic compression with 200 MPa load in a die to produce a sample in the pellet with 8 cm of diameters and 6 cm of thickness. The consolidation process was then carried out by the sintering process using the new apparatus of APS. APS (Arc Plasma Sintering) was the sintering apparatus based on the plasma generated by the electric arc as the heat source. The sintering process was done for 4 minutes with a plasma current of 70 A. An oxidation test was performed on the MSB (Magnetic Suspension Balance) workstation in the air atmosphere at 700°C to simulate the temperature in fuel cladding conditions. The oxidation time was carried out for 8 hours to get insight into the early stage of oxidation. The oxidation characteristic was extracted from the curve describing the relation of the weight gain to the oxidation time.

The addition of ZrO_2 itself, which can affect the crystal structure, has been analyzed the XRD pattern with the Rietveld method using Highscore software. The oxide layer and its effect on the mechanical properties were evaluated based on the microstructure and hardness measurements. An optical microscope and SEM-EDS were used to characterize the microstructure and elemental composition, while the Vickers test was performed to evaluate the hardness of the alloy matrix before and after the oxidation process.

RESULTS AND DISCUSSION

Crystal Structure

All XRD patterns were recorded for characterization at room temperature using the PANalytycal EMPYREAN XRD machine PW1710 type using CuKα radiation. The XRD pattern of 316L powder has the three highest peaks at the diffraction angles 43°, 44°, and 50°, while the ZrO_2 powder at angles 28°, 31°, and 34°, as shown in **Figure 1**. The two samples show significantly different patterns. The 316L substrate has 2 phases presenting diffraction peaks at 43.7°, 50.76°, 74.60°, and 90.60°, which

are consistent with 111, (011), (022), and (113) reflection planes of γ austenite. In contrast, at 44.55°, 64.53°, and 82.0°, the representations of (011), (002), and (003) planes are the peaks of ferrite reflection [10], [11], respectively. However, the XRD pattern of the ZrO_2 material is dominantly identical to the study conducted by Onkar Mangla and Savita Roy [12]
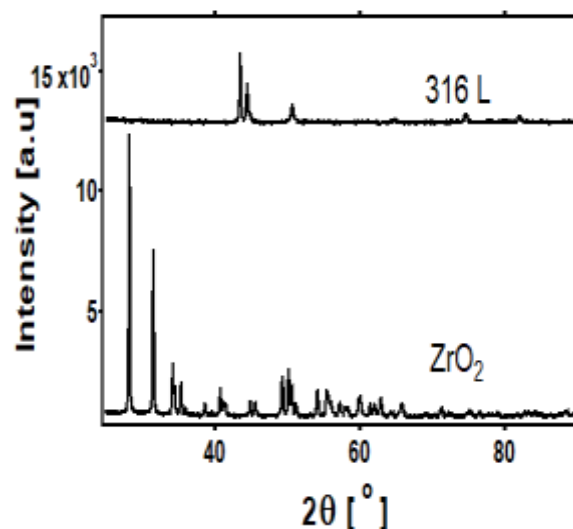
Figure 1. XRD pattern of 316 L and ZrO2 powders.

Several XRD patterns are shown in the figure below for samples of SS 316L (namely 316L steel) and SS 316L + ZrO_2 (namely 316-ODS steel). The presence of Austenite peaks (FCC) and several ferrite peaks (BCC) in the diffractogram pattern for 316L steel makes further discussion in the XRD pattern refinement, as shown in **Figure 2**. The XRD patterns of the 316L and 316L ODS steel samples were refined by the Rietveld method using the Highscore program to obtain austenite and ferrite contents. The initial refinement was determined by the zero point shift parameters, the background, the unit cell, and the inputted austenite and ferrite phases. Meanwhile, the small phase addition of ZrO_2 was not used as input because the peaks of the plane did not exist in the XRD pattern. The austenite phase has referred to the ICSD collection code of 53803 with a space group of Fm-3m, while the ferrite phase was code of 64785 and space group of Im-3m.
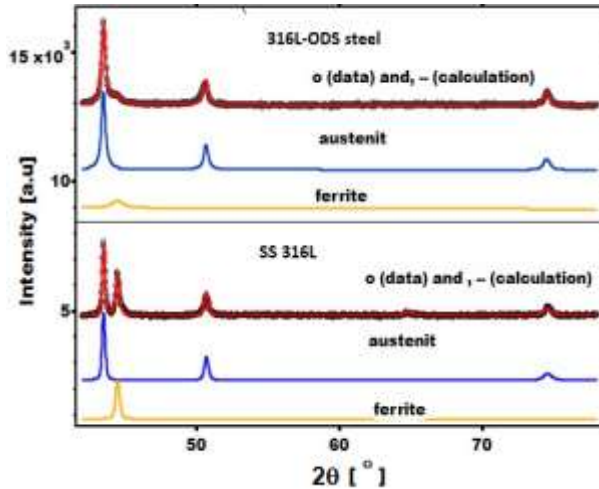
Figure 2. XRD refinement results of 316L and 316L-ODS steel samples. XRD intensity data is labelled with o, total calculations with a red line, austenite with a blue line, and ferrite with a yellow line.

The statistical refinement errors of the R profile and R weighted profile are 2.49521%, 3.32156%, and 2.5051, 3.22117% for 316L and 316l-ODS steel materials, respectively. According to Kniess and Tamer, a value of Rp and Rwp below 10% is a good agreement of this refinement process[13], [14].

Refinement results of the 316L steel sample showed austenite and ferrite contents were 64.7% and 35.3%, while the 316 ODS steel sample was 81.6% and 18.4% in weight, respectively.

Oxidation
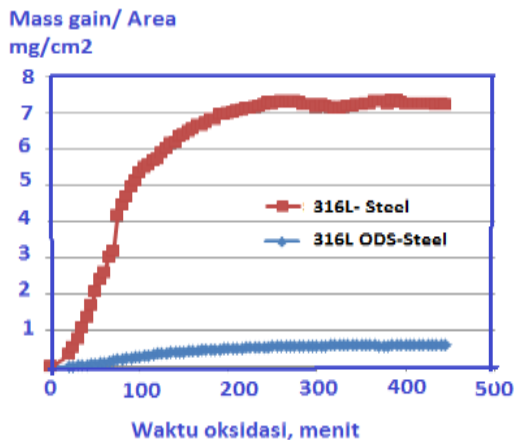
Figure 3. Oxidation characteristic curve of 316L steel and 316L- ODS steel heated at 700°C.

Figure 3 shows the oxidation curves of the SS316L-ODS sample before and after dispersed by the zirconia acquired during the MSB test. The weight gains resulted from the sample oxidation in the air are plotted as a function of the oxidation time.

The oxidation curves of samples during heating up to ca. 150 minutes follow the characteristic of parabolic kinetics. However, the 316L-ODS steel sample shows a lower oxidation rate than those of the 316L steel sample. For the ODS steel 316L, the weight gains of 0.5 mg/cm2 after 180 minutes oxidation time become early constant, while for SS 316L steel, the constant weight gain obtained around 7 mg/ cm2 after 250 minutes oxidation. Some irregularities exist in 316L steel oxidation curves after 300 minutes in the range between 1 to 2 mg/cm2. The characteristic of parabolic kinetics where the mass gain is proportional to the square root of time showed that the oxide formation on both samples oxygen inward diffusion-driven process. This stands in good agreement with the oxidation characteristic of Fe-Cr alloy at high temperatures[15], [16]. The mechanism of high-temperature oxidation of ODS steel alloys is widely accepted to be the diffusion of oxygen anions through the oxide lattice. The metal cations transport, on the other hand, is fully inhibited. The very low corrosion rate of 316L-ODS steel at the beginning of the oxidation can be considered caused by the effect of zirconia dispersed that caused grain coarsening, which decreases the number of oxide crystallites formed the possibilities of oxygen diffusion channelling between the oxide grains. This phenomenon has also been previously observed and reported by Dimyati et al. on the high-temperature FeCrAl alloys [17]. The irregularities of the relative peaks of the mass gain indicate local flacking of small portions of an oxide layer, which quickly reheals and is renewed.

The content of the austenite structure in the ODS-steel material increased from 64.7 to 81.6 wt% in the presence of ZrO_2 dispersion, which affected the slowing down of the corrosion rate, especially before the passivation area. Likewise, the deceleration of oxide corrosion was nearly 14 times for high-temperature ODS steel. ODS steel more clearly showed a lower potential for surface damage than for 316L steel. This is also identical to the comparative corrosion study between austenite and ferrite that has been carried out by Oksiuta et al. [18], [19]. Oxidation characteristics of the austenite material play an important role in resisting corrosion of ODS steel,

as also occurs in the measurement of electrochemical corrosion in the welding area carried out by Vladana et al. [20].

Microstructure

The microstructure of SS316L steel and SS316L-ODS steel synthesized by powder metallurgy process is shown in **Figure 2**. The samples showed a good appearance with little porosity and a good dense structure.

a)

b)
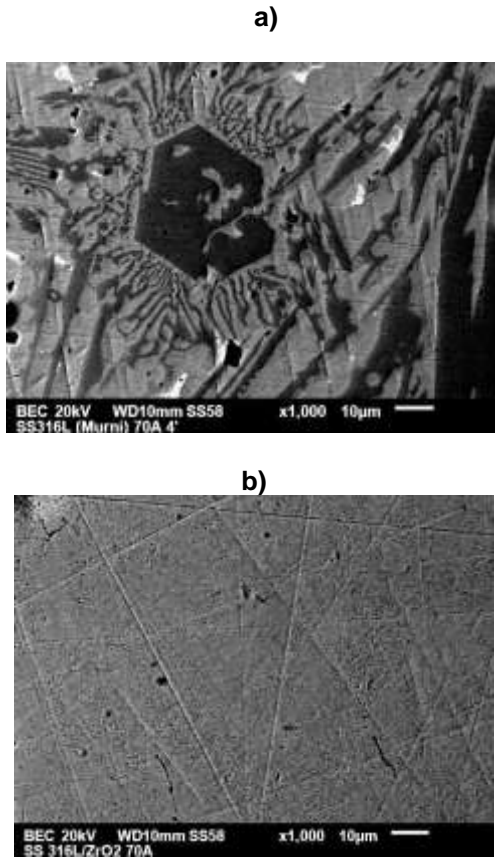
Figure 4. Microstructure of 316L steel (a) and 316L ODS steel (b).

The SEM-EDX examination revealed the presence of particles with different sizes and compositions randomly dispersed in the matrix. Zirconia dispersion in the ODS synthesis of powder metallurgy processing changed the microstructure. Before being dispersed by zirconia, the 316L steel has a lateral structure with some precipitates in the matrix and grain; after synthesizing by powder metallurgy with zirconia dispersion, the structure change to the general appearance of small and equiaxed grains and some elongated grains. The microstructure

change was caused by the main process of ball milling due to the mixing, grain refining, and pre alloying process. Grains and grain boundaries for the ODS steel 316L are difficult to distinguish because of structural characteristics such as the lancet shape of these phases. From the phase analysis, the 316L-ODS steel exhibits the dominant austenitic structure with a little ferritic phase. The microstructure in the cross-section area for both samples of SS 316L and SS316L-ODS steel was shown in **Figure 4**.

a)

b)
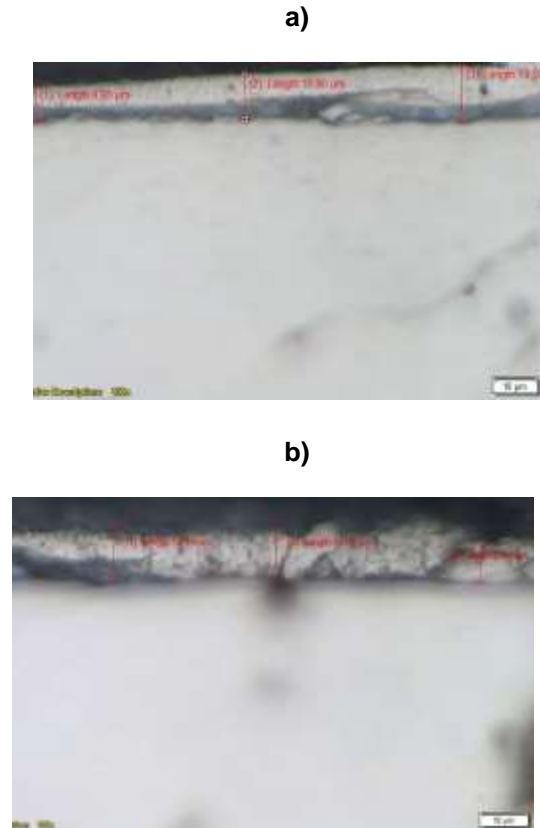
Figure 5. Optical microscope image of SS316L-steel (a) SS316L-ODS steel (b)

From **Figure 5**, the oxide formed on the sample's surface can be observed to consist of many layers as protection from the oxygen attack. The oxide layer thicknesses measured by Optic micrographs of 316L steel and the 316L-ODS steel after oxidation at 700°C have similar layer thicknesses between 10 to 12 μm. In agreement with the result of the MSB test as shown in the oxidation characteristic curve, the oxide layer thickness of SS 316L-ODS steel should be thinner than the layer thickness of 316L steel. However, based on the oxide measurement above, the thickness of the ODS

steel has similar oxide thickness oxide. In addition, some investigation has reported that homogenizing distribution of the zirconia increased the corrosion resistance [21]. Therefore the zirconia dispersion was predicted to influence the formation and composition of the oxide that obtained a superior protected layer with the thicker layer thickness.

Hardness measurement on both sample matrixes showed that the SS316L has 74.647 and increase to 83.234 HVN for 316L ODS steel. The higher hardness of the sample was caused mainly by the second hard phase precipitates of zirconia and by the grain refining during the synthesis process that meets with the microstructure discussed above.

CONCLUSION

The XRD pattern refinement results in the crystal structure analysis showed an increase in the austenite phase content from 64.7 to 81.67 wt% and a decrease in the ferrite phase from 35.3 to 18.33 wt% for before and after dispersing the zirconia of 0.5 wt% to the SS316L steel, respectively, so that it can affect corrosion resistance. 316L-ODS steel showed significantly more corrosion resistance, as seen in the oxidation test results on first heating at 700°C. The effect of zirconia dispersion also changes the structure of the grain refining process. Based on the EDS analysis, the oxide layer formed in the two samples is assumed to be stable ZrO_2 which forms a stable with high adhesion oxide function as layer protection. The hardness of ODS steel has increased considerably low.

AUTHOR INFORMATION

Corresponding Authors
E-mail: idnafahda@gmail.com.
E-mail: bandri@batan.go.id.

ACKNOWLEDGMENTS

REFERENCES

[1] G. Zheng, B. Kelleher, G. Cao, M. Anderson, T. Allen, and K. Sridharan, "Corrosion of 316 stainless steel in high temperature molten Li2BeF4 (FLiBe) salt," J. Nucl. Mater., vol. 461, no. June, pp. 143–150, 2015, DOI: 10.1016/j.jnucmat.2015.03.004.

[2] H. Savaloni, E. Agha-Taheri, and F. Abdi, "On the corrosion resistance of AISI 316L-type stainless steel coated with manganese and annealed with flow of oxygen," J. Theor. Appl. Phys., vol. 10, no. 2, pp. 149–156, 2016, DOI: 10.1007/s40094-016-0213-0.

[3] IAEA, "IAEA Nuclear Energy Series Structural Materials for Liquid Metal Cooled Fast Reactor Fuel Assemblies — Operational Behaviour," IAEA Nucl. Energy Ser., p. 103, 2012.

[4] M. Serrano, A. García-Junceda, R. Hernández, and M. H. Mayoral, "On anisotropy of ferritic ODS alloys," Energy Mater. Mater. Sci. Eng. Energy Syst., vol. 9, no. 3, pp. 1664–1668, 2014, doi: 10.1179/1743284714Y.0000000552.

[5] S. Li et al., "Microstructure and mechanical properties of 16 Cr-ODS ferritic steel for advanced nuclear energy system," J. Phys. Conf. Ser., vol. 419, no. 1, 2013, DOI: 10.1088/1742-6596/419/1/012036.

[6] Q. Zhao et al., "Microstructure and tensile properties of a 14Cr ODS ferritic steel," Mater. Sci. Eng. A, 2017, DOI: 10.1016/j.msea.2016.10.118.

[7] J. Macías-Delgado et al., "Microstructure and tensile properties of ODS ferritic steels mechanically alloyed with Fe2Y," Nucl. Mater. Energy, 2016, DOI: 10.1016/j.nme.2016.09.019.

[8] A. Hotař, P. Kejzlar, M. Palm, and J. Mlnařík, "The effect of Zr on high-temperature oxidation behaviour of Fe3Al-based alloys," Corros. Sci., 2015, DOI: 10.1016/j.corsci.2015.07.016.

[9] J. Rakhmonov, G. Timelli, and F. Bonollo, "The Effect of Transition Elements on High-Temperature Mechanical Properties of Al–Si Foundry Alloys–A Review," Adv. Eng. Mater., vol. 18, no. 7, pp. 1096–1105, 2016, DOI: 10.1002/adem.201500468.

[10] J. L. Cardoso, M. Mandel, L. Krüger, L. F. G. Herculano, P. deLima Neto, and M. J. G. Da Silva, "Corrosion behavior of austenitic stainless steels in CO2-saturated synthetic oil field formation water," Mater. Res., vol.

22, no. 4, pp. 1–11, 2019, DOI: 10.1590/1980-5373-MR-2018-0334.

[11] M. Ziętala et al., "The microstructure, mechanical properties and corrosion resistance of 316 L stainless steel fabricated using laser engineered net shaping," Mater. Sci. Eng. A vol. 677, pp. 1–10, 2016, DOI: 10.1016/j.msea.2016.09.028.

[12] O. Mangla and S. Roy, "Monoclinic Zirconium Oxide Nanostructures Having Tunable Band Gap Synthesized under Extremely Non-Equilibrium Plasma Conditions," Proceedings, vol. 3, no. 1, p. 10, 2018, DOI: 10.3390/iocn_2018-1-05486.

[13] C. T. Kniess, J. C. de Lima, and P. B. Prates, The Quantification of Crystalline Phases in Materials: Applications of Rietveld Method. 2012.

[14] N. Mitra, P. Sarkar, S. Deb, and S. Basu Majumder, "Multiscale Estimation of Elastic Constants of Hydrated Cement," *J. Eng. Mech.*, vol. 145, no. 4, p. 04019014, 2019, DOI: 10.1061/(ASCE)em.1943-7889.0001582

[15] T. Kurniawan, F. A. B. Fauzi, and Y. P. Asmara, "High-temperature oxidation of fe-cr steels in steam condition – A review," Indones. J. Sci. Technol., vol. 1, no. 1, pp. 107–114, 2016, DOI: 10.17509/ijost.v1i1.2217.

[16] Bandriyana, A. H. Ismoyo, T. Sujitno, and A. Dimyati, "Microstructure and oxidation behavior of high strength steel AISI 410 implanted with nitrogen ion," AIP Conf. Proc., vol. 1725, no. April 2016, DOI: 10.1063/1.4945464.

[17] A. Dimyati, H. J. Penkalla, P. Untoro, D. Naumenko, W. J. Quadakkers, and J. Mayer, "High-temperature oxidation of FeCrAl alloys: The effect of Mg incorporation into the alumina scale," Zeitschrift fuer Met. Res. Adv. Tech., 2003, DOI: 10.3139/146.030180.

[18] Z. Oksiuta and E. Och, "Corrosion resistanceof mechanically alloyed 14%cr ODS ferritic steel," Acta Mech. Autom., vol. 7, no. 1, pp. 38–41, 2013, doi: 10.2478/ama-2013-0007.

[19] J. L. Cardoso, M. Mandel, L. Krüger, L. F. G. Herculano,P. deLima Neto, and M. J. G. Da Silva, "Corrosion behavior of austenitic stainless steels in CO2-saturated synthetic oil field formation water," *Mater. Res.*, vol. 22, no. 4, pp. 1–11, 2019, DOI: 10.1590/1980-5373-MR-2018-0334.

[20] V. N. Rajaković-Ognjanović and B. N. Grgur, "Corrosion of an austenite and ferrite stainless steel weld," J. Serbian Chem. Soc., vol. 76, no. 7, pp. 1027–1035, 2011, DOI: 10.2298/JSC100726090R.

[21] H. Li et al., "A new insight into high-temperature oxidation mechanism of super-austenitic stainless steel S32654 in air," J. Alloys Compd., 2016, DOI: 10.1016/j.jallcom.2016.06.023.